



Evaluation of the effect of image noise on CT perfusion measurements using digital perfusion phantoms

Stephan Skornitzke¹ · Jessica Hirsch² · Hans-Ulrich Kauczor¹ · Wolfram Stiller¹

Received: 19 May 2018 / Revised: 5 July 2018 / Accepted: 6 August 2018 / Published online: 11 October 2018
© European Society of Radiology 2018

Abstract

Objectives To assess the influence of image noise on computed tomography (CT) perfusion studies, CT perfusion software algorithms were evaluated for susceptibility to image noise and results applied to clinical perfusion studies.

Methods Digital perfusion phantoms were generated using a published deconvolution model to create time-attenuation curves (TACs) for 16 different combinations of blood flow (BF; 30/60/90/120 ml/100 ml/min) and flow extraction product (FEP; 10/20/30/40 ml/100 ml/min) corresponding to values encountered in clinical studies. TACs were distorted with Gaussian noise at 50 different strengths to approximate image noise, performing 200 repetitions for each noise level. A total of 160,000 TACs were evaluated by measuring BF and FEP with CT perfusion software, comparing results for the maximum slope and Patlak models with those obtained with a deconvolution model. To translate results to clinical practice, data of 23 patients from a CT perfusion study were assessed for image noise, and the accuracy of reported CT perfusion measurements was estimated.

Results Perfusion measurements depend on image noise as means and standard deviations of BF and FEP over repetitions increase with increasing image noise, especially for low BF and FEP values. BF measurements derived by deconvolution show larger standard deviations than those performed with the maximum slope model. Image noise in the evaluated CT perfusion study was 26.46 ± 3.52 HU, indicating possible overestimation of BF by up to 85% in a clinical setting.

Conclusions Measurements of perfusion parameters depend heavily upon the magnitude of image noise, which has to be taken into account during selection of acquisition parameters and interpretation of results, e.g., as a quantitative imaging biomarker.

Key Points

- CT perfusion results depend heavily upon the magnitude of image noise.
- Different CT perfusion models react differently to the presence of image noise.
- Blood flow may be overestimated by 85% in clinical CT perfusion studies.

Keywords Tomography, x-ray computed · Perfusion imaging · Phantoms, imaging · Software · Artifacts

Electronic supplementary material The online version of this article (<https://doi.org/10.1007/s00330-018-5709-3>) contains supplementary material, which is available to authorized users.

✉ Wolfram Stiller
wolfram.stiller@med.uni-heidelberg.de

¹ Diagnostic & Interventional Radiology (DIR), Heidelberg University Hospital, Im Neuenheimer Feld 110, 69120 Heidelberg, Germany

² CHRESTOS Institut, Emil-Figge-Straße 43, 44227 Dortmund, Germany

Abbreviations

AIF	Arterial input function
ANCOVA	Analysis of covariance
BF	Blood flow
CT	Computed tomography
DICOM	Digital Imaging and Communications in Medicine
FEP	Flow extraction product
IRF	Impulse response function
TAC	Time-attenuation curve

Introduction

Computed tomography (CT) perfusion allows non-invasively assessing tissue physiology by performing a dynamic CT acquisition after injection of contrast agent. This functional information on the flow rate or flow extraction product, for example, allows for quantitative assessment of diseases that influence regional blood flow, such as tumors or stroke [1]. Promising results have been obtained in a multitude of studies, showing the potential of CT perfusion for tumor identification or therapy response assessment [2–5].

Because of the required dynamic acquisition, CT perfusion studies are often acquired at comparatively low tube current and potential to limit patient radiation exposure [6, 7]. While studies on the impact of other factors such as contrast agent volume or temporal spacing of the acquisitions on the accuracy of CT perfusion measurements have been performed, no information is available on the influence of the image noise of individual acquisitions [7, 8].

As an alternative to studies using clinical image data, where the ground truth of actual blood flow is unknown and measurements are influenced by noise, digital perfusion phantoms have been proposed, allowing generation of image data from known parameters [9]. With this approach, data can be tailored for each study, avoiding problems of clinical CT perfusion acquisitions, such as radiation exposure to the patients, image noise of unknown magnitude, or patient motion.

The main goal of this study is the use of digital perfusion phantoms to quantitatively evaluate the influence of image noise on the accuracy of CT perfusion measurements performed with two different perfusion models. Furthermore, the results gained using the phantom are applied to retrospectively evaluate results from an earlier CT perfusion study and provide an estimate of the accuracy of measured parameters. In all, the aim is to improve the choice of acquisition protocols for future CT perfusion studies by investigating the connection between image noise and measurement accuracy.

Materials and methods

Digital perfusion phantoms

A digital perfusion phantom is a digitally generated image series that mimics some or all aspects of a regular CT perfusion acquisition. This image data can be evaluated using CT perfusion software, allowing for comparison of the results against the parameters used to generate the phantom (i.e., the ground truth), thus providing a detailed assessment of the capabilities of the software and the implemented perfusion models [9]. The process to create a digital perfusion phantom is described in detail in the [Electronic Supplementary Material](#).

A total of 16 phantoms were generated for a total of 16 combinations of the parameters blood flow (BF: 30, 60, 90 and 120 ml/100 ml/min) and flow extraction product (FEP: 10, 20, 30 and 40 ml/100 ml/min). Parameters were chosen to match results observed in clinical studies (see Table 1) [2, 3, 5, 6, 10–12]. Time to start and mean transit time were both set to 5 s, and the temporal spacing between images was set to 1 s for a total acquisition time of 45 s.

Each of the phantoms contains 10,000 time-attenuation curves (TACs), corresponding to 50 different noise levels with a standard deviation of $\sigma = 0$ HU to $\sigma = 49$ HU. This results in 200 evaluated TACs for each combination of parameters and noise level and a grand total of 160,000 individual measurements.

Evaluation

Digital perfusion phantoms were evaluated using commercially available CT perfusion software (syngo.via VB10B Body Perfusion; Siemens Healthineers). Smoothing strength was set to 0 mm, and the following parameter maps were calculated and exported in DICOM format:

- BF (maximum slope model) [13]
- BF (deconvolution model) [10]
- FEP (Patlak model) [14]
- FEP (deconvolution model) [10]

Figure 1 shows an example of resulting parameter maps. Parameter maps were evaluated using software developed in-house, automatically determining BF and FEP for each TAC from the results exported from the commercial software.

Statistical analysis

For descriptive analysis, means and standard deviations of BF and FEP were calculated for each combination of BF, FEP and noise level, i.e., results were averaged over the 200 repetitions.

For statistical analysis, the data sets for each evaluated perfusion parameter (BF or FEP) containing 320,000 observations (160,000 TACs evaluated with two perfusion models, either deconvolution or maximum slope/Patlak) were evaluated by performing an analysis of covariance (ANCOVA) using SAS 9.4 (SAS Institute). In detail, the type of perfusion model was modeled as a classifier, while the ground truths for BF, FEP and noise level were modeled as covariates for the prediction of the measurement (either BF or FEP).

The ANCOVA was performed in a multi-step process, initially considering all main effects as stated above and all interactions between those effects. In an iterative process, effects that were not considered significant at a level of $\alpha = 0.05$ using type II sum of squares and not part of significant interaction effects were omitted from the ANCOVA until no more effects could be omitted. Because of the large number of tests (15 tests for first-

Table 1 Overview of measured perfusion parameters and acquisition parameters reported in the literature. Where available, acquisition parameters are tabulated in terms of tube potential, tube current-time product, scan coverage and number of dynamic acquisitions.

Depending on the data given in the respective publications, corresponding radiation exposure of the CT perfusion examination is stated in terms of dose-length product (DLP in [mGy·cm]) and/or effective dose (in [mSv])

Author	Organ	Measurement location	Blood flow ^a ml/100 g/min ^b ml/100 ml/min	Flow-extraction product/ permeability ^a ml/100 g/min ^b ml/100 ml/min	Acquisition parameters	Radiation exposure ^a DLP ^b effective dose
Abels et al [10]	Brain	Gray matter White matter Infarct core	65 ± 4.7 ^a 30 ± 2.7 ^a 12 ± 4.2 ^a	N/A	80 kV _p 180–235 mAs N/A 40 acq.	N/A
Fritz et al [5]	Pancreas	Recurrence tissue Postoperative soft-tissue	16.6 ± 6.0 ^b 24.7 ± 18.1 ^b	8.7 ± 4.0 ^b 10.7 ± 9.3 ^b	Sn 140/80 kV _p 104/270 mAs ~ 19 mm 34 acq.	599 mGy·cm ^a 9.0 mSv ^b
Jiang et al [2]	Liver	HCC baseline Post-treatment	108.47 ± 85.85 ^a 55.25 ± 34.65 ^a	34.02 ± 14.29 ^a 21.34 ± 7.3 ^a	100–120 kV _p 200–240 mAs N/A 25–30 acq.	N/A
Kaufmann et al [3]	Liver	HCC	68.3 ^b	33.8 ^b	80 kV _p 100/120 mAs 69–97 mm 26 acq.	7 mSv ^b
Klauss et al [11]	Pancreas	Carcinoma Parenchyma	27 ± 20 ^a 89 ± 19 ^a	21 ± 10 ^a 37 ± 8 ^a	140/80 kV _p 50/270 mAs ~ 17 mm 34 acq.	427 mGy·cm ^a 6.4 mSv ^b
Li et al [6]	Pancreas	Carcinoma Parenchyma	33.89 ± 12.48 ^a 99.49 ± 15.23 ^a	31.26 ± 15.29 ^a 28.63 ± 10.01 ^a	70 kV _p 120 mAs or 80 kV _p 100 mAs 70 mm 24 acq.	246 or 325 mGy·cm ^a 3.6 or 4.9 mSv ^b
Schneeweiß et al [12]	Pancreas	Carcinoma	36.9 ± 16.0 ^b	12.4 ± 8.2 ^b	80 kV _p 100/120 mAs 69 mm 26 acq.	7 mSv ^b

step ANCOVA), the Bonferroni-Holm correction was used to adjust significance levels ($\alpha = 0.05$) for multiple testing.

Pearson's correlation coefficient was calculated for the linear correlation between results obtained by the different perfusion models using Excel 2016 (Microsoft Corp.).

Comparison to clinical data

The results obtained with the digital perfusion phantom were used to retrospectively analyze data from an earlier CT perfusion study of pancreatic carcinoma to estimate the accuracy of the perfusion measurements [15]. Patients gave written informed consent for inclusion in the study, approval of the institutional review board was obtained, and guidelines from the World Medical Association were followed (Declaration of Helsinki 2013).

In this earlier study, 23 patients were scanned with a DECT perfusion protocol after injection of 80 ml of contrast agent, and data from 80-kV_p images were used to measure tissue perfusion. Images were acquired at 80 kV_p/140 kV_p with tin filtration using dual-source DECT and tube current modulation with reference values of 270/104 mAs, as previously reported [15].

Image noise of the perfusion acquisitions was estimated by evaluating standard deviation of Hounsfield units determined by ROI measurements performed for the first image of the first acquisition of the CT perfusion series. As a robust approximation to the image noise of abdominal CT, ROIs of 250 mm² area were placed in the liver (see Fig. 2a). Two patients were excluded from the evaluation as not enough liver tissue was included in the acquisition.

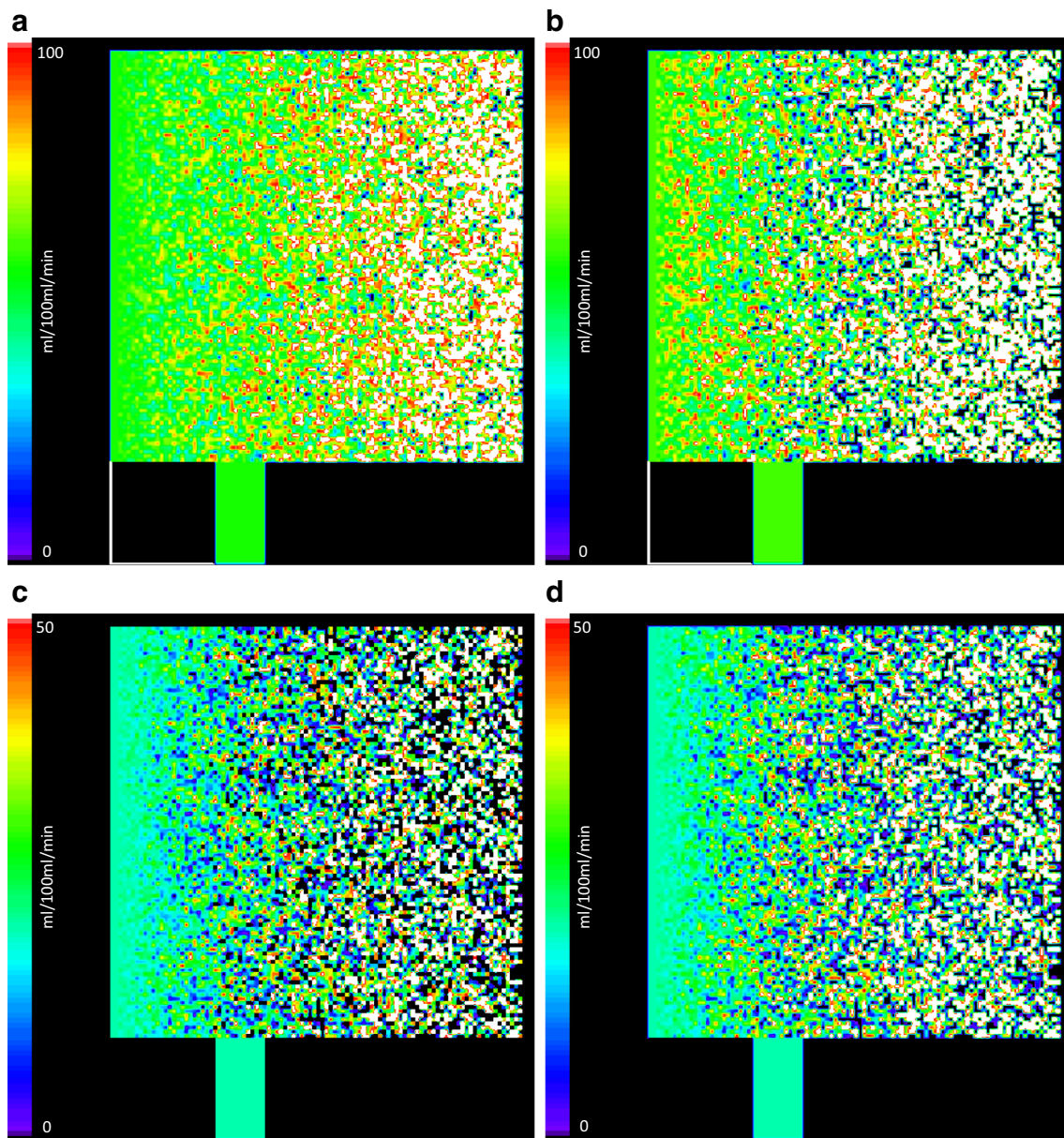


Fig. 1 Example of the parameter maps calculated for a digital perfusion phantom using commercially available CT perfusion software (syngo.via Body perfusion VB10B, Siemens Healthineers). The ground truth for the shown phantom is blood flow = 60 ml/100 ml/min and flow extraction product = 20 ml/100 ml/min. Top left (a): Blood flow (maximum slope

model). Top right (b): Blood flow (deconvolution model). Bottom left (c): Flow extraction product (Patlak model). Bottom right (d): Flow extraction product (deconvolution model). Note the increase in very high and very low measurements for all models with increasing noise level and the notable difference between the two parameter maps of blood flow

Descriptive statistics of standard deviation determined by ROI measurements were calculated and used to estimate the accuracy of the previously reported CT perfusion measurements based on the results of the digital perfusion phantom.

Results

Parameter maps could be calculated using the commercially available CT perfusion software for all perfusion phantoms, and all 160,000 TACs could be evaluated. Parameter maps

calculated with the Patlak model reported negative values for FEP in 6.35% of the TACs (10,162/160,000). For further analysis, these values were treated as a value of zero.

For BF, an increase in image noise leads to an increase in mean measured values for both models (see Fig. 3). The increase is larger for smaller BF values and nearly vanishes at 120 ml/100 ml/min. Furthermore, an increase in image noise leads to an increase in the standard deviation of the measured values for both perfusion models, and the standard deviation is higher for measurements with the deconvolution model than for those with the maximum slope model. In general, a

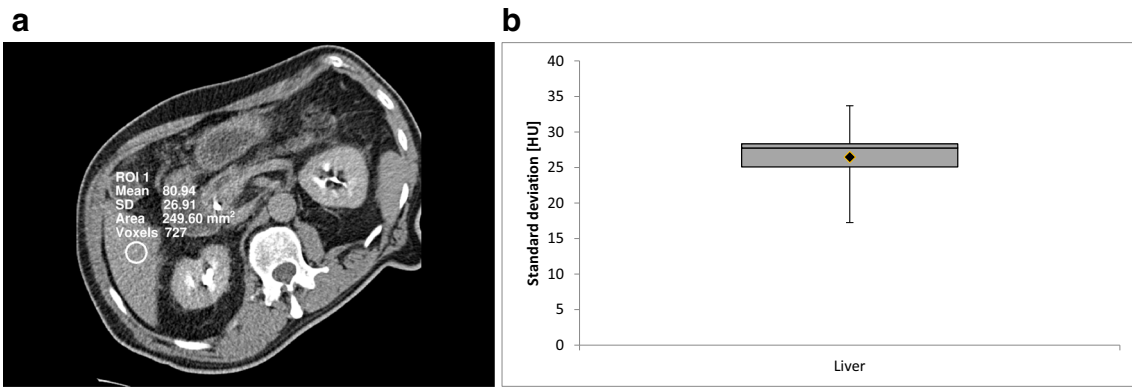


Fig. 2 Left (a): Estimating image noise for a CT perfusion study by measuring the standard deviation of Hounsfield numbers in a region of interest placed in the liver. Right (b): Descriptive statistics of measured standard deviations (image noise)

dependence of the reported BF on FEP can be observed (see Table 2). Figure 3 shows means and standard deviations of measured BF when averaging over different FEP values.

Similar to BF, an increase in image noise leads to an increase in mean measured values of FEP for both models (see Fig. 4). The increase is yet again larger for smaller FEP values and nearly vanishes at 40 ml/100 ml/min. A larger increase in mean values can be observed when using the deconvolution model compared with the Patlak model. Again, the standard deviation increases with increasing image noise for both perfusion models. In general, measurements of FEP show a dependence on BF values (see Table 3). Figure 4 shows means and standard deviations of FEP when averaging over different BF values.

Correlation between BF measured with the deconvolution and the maximum slope models is moderate ($r = 0.63$) when comparing all measured values (i.e., all repetitions). Correlation is very high ($r = 0.97$) when comparing mean values averaged over all repetitions. For measurements of FEP, correlation between values measured with both models is very high in both cases ($r = 0.95$ and $r = 0.97$).

All calculated ANCOVA models were statistically significant ($p < 0.0001$). Tables 4 and 5 show the final summary of all effects that are significant or that are part of a significant interaction for both evaluations. For BF, all main effects are statistically significant, while for FEP, the perfusion model was only significant as

part of interaction effects: of the effects including an interaction with the perfusion model, only the interaction of the ground truth of BF, noise level and perfusion model was reported as significant.

For the evaluated clinical CT perfusion acquisitions, mean CT numbers measured in the liver averaged for all patients were 74.21 HU, and the averaged standard deviation was 26.4 HU (see Fig. 2b). Previously reported blood flow was 87.6 ± 28.4 ml/100 ml/min for healthy pancreatic tissue and 38.6 ± 22.2 ml/100 ml/min for carcinoma [15]. For the digital perfusion phantom evaluated with the deconvolution model, a standard deviation of 26.4 HU resulted in a relative difference of 85.4%/20.7%/4.9%/-1.8% to the ground truth of blood flow (30/60/90/120 ml/100 ml/min, respectively).

Discussion

The main goal of this study was to evaluate perfusion models regarding their performance in the presence of image noise and to estimate the accuracy of clinical CT perfusion measurements. As expected, results show a significant dependence of measurements of BF and FEP on image noise levels, independent of the perfusion model used. With increasing image noise, perfusion parameters are overestimated. This effect is more prominent for low levels of BF or FEP, where the mean value of the

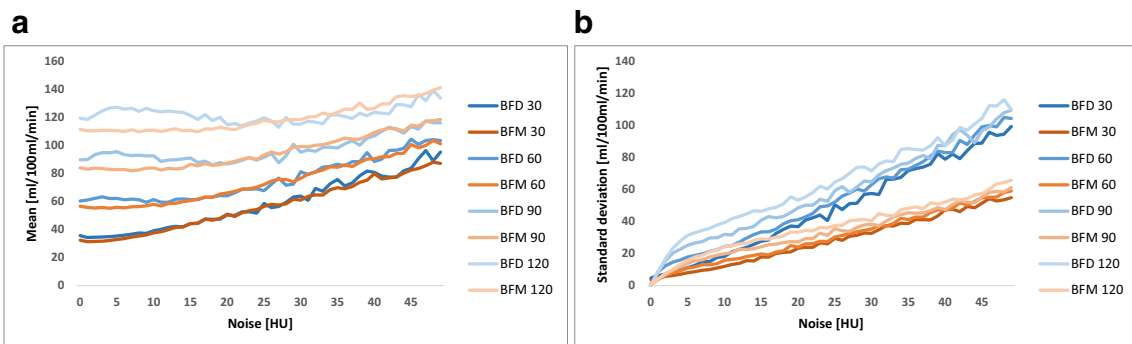


Fig. 3 Comparison of measurements of blood flow using the maximum slope model (BFM) and deconvolution model (BFD) when averaging over all repetitions and different levels of flow extraction product for

the ground truth values of blood flow (30/60/90/120 ml/100 ml/min). Left (a): Mean values. Right (b): Standard deviations

Table 2 Mean values \pm standard deviation for measurements of blood flow (BF) with the maximum slope and deconvolution model averaged over all noise levels for the different ground truth (GT) values of BF and flow extraction product (FEP)

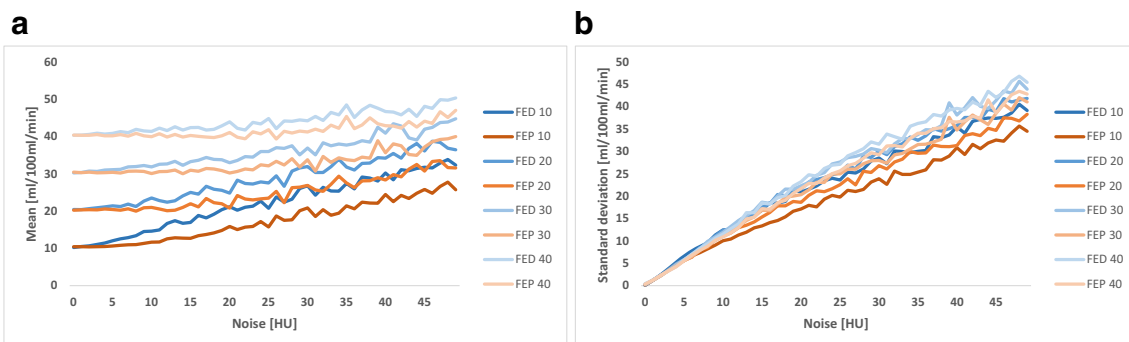
BF measured with maximum slope model (ml/100 ml/min)				
GT FEP	10 ml/100 ml/min	20 ml/100 ml/min	30 ml/100 ml/min	40 ml/100 ml/min
GT BF				
30 ml/100 ml/min	51.90 \pm 39.69	53.36 \pm 36.25	57.37 \pm 36.25	62.78 \pm 34.11
60 ml/100 ml/min	71.50 \pm 40.23	73.07 \pm 37.77	74.41 \pm 36.90	76.29 \pm 35.54
90 ml/100 ml/min	94.54 \pm 41.48	94.84 \pm 39.25	97.99 \pm 37.71	96.70 \pm 35.77
120 ml/100 ml/min	118.14 \pm 43.70	118.48 \pm 41.55	119.70 \pm 40.60	120.76 \pm 39.10
BF measured with deconvolution model (ml/100 ml/min)				
GT FEP	10 ml/100 ml/min	20 ml/100 ml/min	30 ml/100 ml/min	40 ml/100 ml/min
GT BF				
30 ml/100 ml/min	54.29 \pm 64.63	55.81 \pm 60.64	59.14 \pm 57.83	63.91 \pm 53.29
60 ml/100 ml/min	71.72 \pm 66.03	75.35 \pm 64.13	76.16 \pm 61.36	79.05 \pm 57.94
90 ml/100 ml/min	94.71 \pm 68.81	96.76 \pm 66.33	98.52 \pm 64.78	98.94 \pm 59.68
120 ml/100 ml/min	119.95 \pm 75.74	121.37 \pm 71.34	123.56 \pm 68.63	125.19 \pm 65.64

measurements exceeds the ground truth by a factor of two for noise levels above 40 HU. This overestimation may in part be explained by the fact that both BF and FEP offer no physiologically meaningful explanation for values below zero. Therefore, values below zero are truncated (i.e., set to zero) by all commonly used perfusion software, thus resulting in an increase in means when the variance of the measurement increases.

Comparing the evaluated perfusion models, both descriptive statistics and statistical analysis show a difference in calculated BF values when image noise increases. Furthermore, BF values calculated with the maximum slope model show a lower standard deviation than those calculated with the deconvolution model and might therefore be more reliable and less susceptible to image noise. For FEP, the difference in measurements between both models was not statistically significant, but the interpretation of statistical results in the presence of interaction effects is complicated. Considering correlation between the models, results are in agreement with earlier studies using clinical image data, showing moderate to very high correlation for measurements of BF and FEP [3, 12].

Employing results obtained from the digital perfusion phantom to clinical CT perfusion measurements allows estimating the accuracy of these measurements. Disregarding additional filtering of the perfusion maps and averaging during ROI evaluations, the results show that measurements in healthy pancreatic tissue can be regarded as accurate despite image noise while quantitative evaluations of measurements in pancreatic carcinoma have to be treated with caution. Considering the reported blood flow of 38.6 ± 22.2 ml/100 ml/min and the estimated relative difference to ground truth of 85.4%, it is likely that the actual blood flow in pancreatic carcinoma is even lower than perfusion measurements indicate.

Furthermore, the results of this study can be applied to published CT perfusion studies. From the studies listed in Table 1, it is evident that performing measurements in healthy pancreas can be expected to yield flow values in the order of 100 ml/100 ml/min, which results in a relatively small influence of image noise on the measurement. However, measurements in pancreatic lesions yield much lower blood flow values, meaning measurements are much more susceptible to image noise and

**Fig. 4** Comparison of measurements of flow extraction product using the Patlak model (FEP) and deconvolution model (FED) when averaging over all repetitions and different levels of blood flow for the ground truth

values of the flow extraction product (10/20/30/40 ml/100 ml/min). Left (a): Mean values. Right (b): Standard deviations

Table 3 Mean values ± standard deviation for measurements of the flow extraction product (FEP) with the Patlak and deconvolution models averaged over all noise levels for the different ground truth (GT) values of FEP and blood flow (BF)

FEP measured with the Patlak model (ml/100 ml/min)					
GT FEP	10 ml/100 ml/min	20 ml/100 ml/min	30 ml/100 ml/min	40 ml/100 ml/min	
GT BF					
30 ml/100 ml/min	16.31 ± 21.04	23.56 ± 22.67	31.77 ± 25.01	39.96 ± 25.79	
60 ml/100 ml/min	16.75 ± 21.61	24.69 ± 24.26	32.72 ± 25.49	41.57 ± 26.55	
90 ml/100 ml/min	17.90 ± 22.68	25.37 ± 24.71	33.57 ± 26.65	42.17 ± 27.56	
120 ml/100 ml/min	18.17 ± 23.44	25.72 ± 25.47	33.89 ± 27.03	42.93 ± 28.24	
FEP measured with deconvolution model (ml/100 ml/min)					
GT FEP	10 ml/100 ml/min	20 ml/100 ml/min	30 ml/100 ml/min	40 ml/100 ml/min	
GT BF					
30 ml/100 ml/min	18.36 ± 22.81	24.88 ± 24.03	32.89 ± 26.48	40.70 ± 27.48	
60 ml/100 ml/min	20.54 ± 24.69	27.52 ± 26.38	34.97 ± 27.11	43.44 ± 28.00	
90 ml/100 ml/min	23.54 ± 27.44	30.00 ± 28.26	37.31 ± 29.07	45.17 ± 29.35	
120 ml/100 ml/min	25.40 ± 29.78	31.51 ± 30.10	38.97 ± 30.66	47.20 ± 31.08	

can therefore be expected to be overestimated based on the results of this study. As discussed above, differences in blood flow between tissue types might consequently be larger than they appear. Similar effects may also be observed for other organs and pathologies, which would have to be analyzed in a comprehensive literature review.

In general, CT perfusion acquisitions at reduced dose might overestimate perfusion parameters and reductions in patient radiation exposure might come at reduced measurement

accuracy. As the effect of image noise is much more prominent for low BF and FEP values, differences in perfusion parameters between tissue types might be larger than estimated and the ability to differentiate between tissue types might be reduced.

In clinical practice, the expected image noise of individual acquisitions should be taken into account during the selection of acquisition parameters for CT perfusion studies. For the digital perfusion phantoms, results within 50% of the ground truth could only be achieved when limiting image noise to

Table 4 Results of the final stage of the analysis of covariance (ANCOVA) for the parameter blood flow; main effects were ground truth of the *blood flow* and *flow extraction product*, *perfusion model* used for the evaluation and *noise level*, and all interactions between these main effects were included. Only effects from the final stage model are shown, i.e., statistically significant effects or effects that are part of a significant interaction effect. Interaction effects are denominated by an asterisk (*) between individual effects

ANCOVA: blood flow					
Effect	Degrees of freedom	Type II sum of squares	Mean square	F value	Reported p value
Blood flow	1	17,654,675	17,654,675	6648.0	0.0001
Flow extraction product	1	416,007	416,007	156.7	0.0001
Noise level	1	5,332,030	5,332,030	2007.8	0.0001
Perfusion model	1	100,971	100,971	38.0	0.0001
Blood flow *	1	230,177	230,177	86.7	0.0001
Flow extraction product					
Blood flow *	1	1,893,557	1,893,557	713.0	0.0001
Noise level					
Blood flow *	1	651,528	651,528	245.3	0.0001
Perfusion model					
Flow extraction product *	1	32,900	32,900	12.4	0.0004
Noise level					
Noise level *	1	202,229	202,229	76.2	0.0001
Perfusion model					
Blood flow *	1	746,675	746,675	281.2	0.0001
Noise level*					
Perfusion model					
Blood flow *	1	68,046	68,046	25.6	0.0001
Flow extraction product *					
Noise level					

Table 5 Results of the final stage of the analysis of covariance (ANCOVA) for the parameter flow extraction product; main effects were ground truth of the *blood flow* and *flow extraction product*, *perfusion model* used for the evaluation and *noise level*, and all interactions between these main effects were included. Only effects from the final stage model are shown, i.e., statistically significant effects or effects that are part of a significant interaction effect. Interaction effects are denominated by an asterisk (*) between individual effects

ANCOVA: flow extraction product					
Effect	Degrees of freedom	Type II sum of squares	Mean square	F value	Reported <i>p</i> value
Blood flow	1	17,074	17,074	25.2	0.0001
Flow extraction product	1	10,448,543	10,448,543	15,418.8	0.0001
Noise level	1	995,970	995,970	1469.7	0.0001
Perfusion model	1	747	747	1.1	0.2937
Blood flow *	1	161,278	161,278	238.0	0.0001
Noise level	1	1206	1206	1.8	0.1821
Blood flow *	1	1206	1206	1.8	0.1821
Perfusion model	1	735,994	735,994	1086.1	0.0001
Flow extraction product *	1	735,994	735,994	1086.1	0.0001
Noise level	1	1731	1731	2.6	0.1099
Noise level *	1	1731	1731	2.6	0.1099
Perfusion model	1	52,249	52,249	77.1	0.0001
Blood flow *	1	52,249	52,249	77.1	0.0001
Noise level *	1	52,249	52,249	77.1	0.0001
Perfusion model	1	52,249	52,249	77.1	0.0001

below 20 HU (BF) and below 10 HU (FEP). An estimation of acquisition parameters in terms of combinations of tube potential (kV_p) and tube current-time product (mAs) to obtain these levels of image noise is displayed in Fig. 5. However, further parameters, such as reconstruction algorithms and kernels, the resulting contrast-to-noise ratio or patient size, have to be considered to provide definitive recommendations for acquisition settings. Still, Fig. 5 illustrates the difficulty in achieving acceptable noise levels and reliable measurements at acceptable levels of patient radiation exposure.

Future CT perfusion studies should take care to report the average image noise of the acquisitions, because of its impact on the accuracy of measured perfusion values. For follow-up studies that perform repeated perfusion measurements for

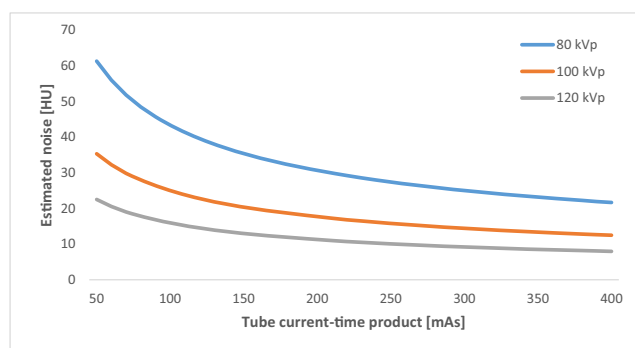


Fig. 5 Estimation of image noise (approximated by standard deviation) for different combinations of tube potential and tube current-time product, extrapolated from the evaluated CT perfusion study. Note that other factors may influence image noise and are not accounted for, e.g., reconstruction kernels, iterative reconstruction, reconstructed slice thickness, primary collimation or other scanner hardware factors

assessing disease progress or therapy response, the impact of systematic overestimation of perfusion parameters can be reduced by keeping acquisition parameters constant between acquisitions, leading to similar noise levels of comparable magnitude. The increase in measurement variance with increasing image noise may be reduced by image post-processing filters, which in turn reduce spatial resolution. In any case, a compromise has to be made between measurement accuracy and patient radiation exposure.

Limitations

The evaluation in this study was focused on only two parameters, BF and FEP, while omitting other parameters such as blood volume or mean transit time. As the total number of parameter sets grows exponentially with the number of parameters, the inclusion of blood volume, for example, as an additional parameter in this study would have quadrupled the number of necessary evaluations, which was not deemed feasible.

Furthermore, only the effect of image noise on TACs was considered in this study, while in a clinical setting the AIF will also be affected. In contrast to TACs, measurements of the AIF are usually averaged over a region of interest, which will reduce the influence of image noise. Nonetheless, preliminary measurements show that a noisy AIF will also affect perfusion measurements. In practice, the evaluation of the effect of noise in the AIF is limited by the use of commercially available CT perfusion software. With the digital perfusion phantoms used in this study, 10,000 TACs can be evaluated simultaneously, while only one AIF can be evaluated at a time. In consequence, it is not feasible to evaluate AIFs in this manner.

Evaluations in this study were only based on the commercial implementation of perfusion models by one vendor. However, this allows comparing the results obtained with the two models without correcting for differences introduced by different implementations of perfusion models by different manufacturers. Nevertheless, similar results can be expected for other vendors.

Conclusion

Accuracy of perfusion parameters measured in the presence of image noise depends heavily on the magnitude of the image noise. Independent of the evaluated perfusion model, image noise will lead to an overestimation of perfusion parameters. Furthermore, different perfusion models are influenced differently by image noise, and the deconvolution-based model shows a larger standard deviation in the presence of image noise than a maximum slope model. In light of the results presented here, the anticipated image noise should be taken into account when selecting acquisition parameters for CT perfusion studies. Based on the outcome of this study, aiming for an image noise of each individual acquisition of below 20 HU (BF) and below 10 HU (FEP) should allow to limit deviation of measured parameters from ground truth to below 50% in conditions similar to the ones evaluated here, regardless of the perfusion model. Furthermore, when performing repeated perfusion measurements, e.g., before and after treatment, one should aim to keep image noise constant to improve the comparability of results.

Funding The authors state that this work has not received any funding.

Compliance with ethical standards

Guarantor The scientific guarantor of this publication is Dr. Wolfram Stiller.

Conflict of interest The authors of this manuscript declare relationships with the following companies: Hans-Ulrich Kauczor is the recipient of a research grant from Siemens Healthineers.

Otherwise, the remaining authors of this manuscript declare no relationships with any companies, whose products or services may be related to the subject matter of the article.

Statistics and biometry Two of the authors have significant statistical expertise:

Dr. Jessica Hirsch (CHRESTOS Institute, Dortmund, Germany) and Dr. Stephan Skornitzke (Heidelberg University Hospital, Diagnostic & Interventional Radiology [DIR], Heidelberg, Germany) have significant statistical expertise and jointly performed the statistical evaluation for this study.

Informed consent Written informed consent was obtained from all subjects (patients) in this study.

Ethical approval Institutional Review Board approval was obtained.

Study subjects or cohorts overlap Some study subjects or cohorts have been previously reported in:

Skornitzke S, Fritz F, Mayer P, Koell M, Hansen J, Pahn G, Hackert T, Kauczor HU, Stiller W. “Dual-energy CT iodine maps as an alternative quantitative imaging biomarker to abdominal CT perfusion: determination of appropriate trigger delays for acquisition using bolus tracking.” *Br J Radiol* 2018; 91: 20170351. doi: 10.1259/bjr.20170351.

Methodology

- not applicable/retrospective
- experimental
- performed at one institution

References

1. Kim SH, Kamaya A, Willmann JK (2014) CT perfusion of the liver: principles and applications in oncology. *Radiology* 272:322–344
2. Jiang T, Kambadakone A, Kulkarni NM, Zhu AX, Sahani DV (2012) Monitoring response to antiangiogenic treatment and predicting outcomes in advanced hepatocellular carcinoma using image biomarkers, CT perfusion, tumor density, and tumor size (RECIST). *Invest Radiol* 47:11–17
3. Kaufmann S, Horger T, Oelker A et al (2015) Characterization of hepatocellular carcinoma (HCC) lesions using a novel CT-based volume perfusion (VPCT) technique. *Eur J Radiol* 84:1029–1035
4. Miles KA, Griffiths MR (2003) Perfusion CT: a worthwhile enhancement? *Br J Radiol* 76:220–231
5. Fritz F, Skornitzke S, Hackert T et al (2016) Dual-energy perfusion-CT in recurrent pancreatic cancer – preliminary results. *Rofo* 188: 559–565
6. Li HO, Sun C, Xu ZD et al (2014) Low-dose whole organ CT perfusion of the pancreas: preliminary study. *Abdom Imaging* 39: 40–47
7. Miles K, Lee TY, Goh V et al (2012) Current status and guidelines for the assessment of tumour vascular support with dynamic contrast-enhanced computed tomography. *Eur Radiol* 22:1430–1441
8. Kandel SM, Meyer H, Boehnert M, Hoppel B, Paul NS, Rogalla P (2014) How influential is the duration of contrast material bolus injection in perfusion CT? Evaluation in a swine model. *Radiology* 270:125–130
9. Pinykh OS (2012) Digital perfusion phantoms for visual perfusion validation. *AJR Am J Roentgenol* 199:627–634
10. Abels B, Klotz E, Tomandl BF, Kloska SP, Lell MM (2010) Perfusion CT in acute ischemic stroke: a qualitative and quantitative comparison of deconvolution and maximum slope approach. *AJNR Am J Neuroradiol* 31:1690–1698
11. Klauss M, Stiller W, Fritz F et al (2012) Computed tomography perfusion analysis of pancreatic carcinoma. *J Comput Assist Tomogr* 36:237–242
12. Schneeweiß S, Horger M, Grözinger A et al (2016) CT-perfusion measurements in pancreatic carcinoma with different kinetic models: Is there a chance for tumour grading based on functional parameters? *Cancer Imaging* 16:43
13. Miles K (1991) Measurement of tissue perfusion by dynamic computed tomography. *Br J Radiol* 64:409–412
14. Patlak CS, Blasberg RG, Fenstermacher JD (1983) Graphical evaluation of blood-to-brain transfer constants from multiple-time uptake data. *J Cereb Blood Flow Metab* 3:1–7
15. Skornitzke S, Fritz F, Mayer P et al (2018) Dual-energy CT iodine maps as an alternative quantitative imaging biomarker to abdominal CT perfusion: determination of appropriate trigger delays for acquisition using bolus tracking. *Br J Radiol* 91:20170351